12th International Conference on Fracture Mechanics of Concrete and Concrete Structures
FraMCoS-12
B.L.A. Pichler, Ch. Hellmich, P. Preinstorfer (Eds)

https://doi.org/10.21012/FC12.1151
MS13-2:2

FAILURE BEHAVIOR OF RC BEAMS BY MEANS OF 3D CONCRETE PRINTING

MINORU KUNIEDA[*], SHUNYA TO[†] TATSUYOSHI KATO[†] AND AKIRA MIYAJIMA[†]

[*] Department of Civil Engineering, Gifu University
1-1 Yanagido, Gifu 501-1193 Gifu, Japan
e-mail: kunieda.minoru.r3@f.gifu-u.ac.jp

[†] Graduate School of Natural Science and Technology, Gifu University
1-1 Yanagido, Gifu 501-1193 Gifu, Japan

Key words: 3D Concrete Printing, Reinforced Concrete, Failure Behavior

Abstract: Flexural tests were conducted on RC beams by using material extrusion 3D printing technology. The used mortar does not include any fibers, and the beams have horizontal and vertical interlayers. It was clarified that the compensation plane was maintained within the cross section, the neutral axis rose with the propagation of flexural cracks. The strain of the mortar at the extreme fiber in compression was about 3000 micron, and flexural failure with interlayer delamination in compression zone was observed finally. In addition, delamination of multiple filament interlayer was observed at the rebar position. The interlayer bond strength was measured and found to be about 30% of the splitting tensile strength of mortar itself.

1 INTRODUCTION

In recent years, many examples of construction using 3D concrete printing (3DCP) technology have been introduced in China, the Middle East, and Europe [1-2]. Japan is one of the world's leading earthquake-prone countries, and structural design for concrete structures by 3DCP technology is necessary.

Efforts to develop 3DCP are accelerating through a joint effort of industry, government, and academia, such as the Japan Concrete Institute, and the Japan Society of Civil Engineers. It is expected that structural members reinforced with rebars will be used, and it is necessary to accumulate knowledge about the fracture of structural members.

This study experimentally verified the flexural failure behavior of beams with axial rebar, which were fabricated using 3DCP. The effect of the interlayer bond strength on failure behavior of the beams were investigated.

2 OUTLINE OF EXPERIMENT

2.1 Printer

The 3D printer used in this study is shown in Fig. 1. The printing system in this study is consist of a six-axis robot arm and a rotary volumetric uniaxial eccentric screw pump. The pump was chosen to deliver a constant amount without pulsation. In addition, a stainless steel cylindrical pipe with a diameter of 25 mm is attached as the discharge nozzle.

2.2 Mortar

Many studies used mortar with short fiber mixed in it [3]. In this study, mortar without fiber was used, because use of a rebar is expected and cost reduction is also required. Mix proportions of mortar [4] are shown in Table 1. The water-to-binder ratio (W/B) was set to 32.2%, and the used binders were high-early-strength Portland cement, additive (fly ash type II), an ettringite-lime composite

Figure 1: 3D printer.

Table 1: Mix proportions of used mortar

Unit content(kg/m^3)					
Water	Cement	Fly ash	Expansive agent	Silica sand	Ad.
336	720	310	20	720	1.4

expansive agent, and silica sand with a fine aggregate binder ratio (S/B) of 69%. In addition, a lignin sulfonate-based AE water reducing agent was used as a chemical admixture. Flow value of mortar according to JIS R 5021 was controlled to be 160 ± 5 mm. The air content at fresh state was 1.1%.

2.3 Beam specimen

The dimensions of the specimen were planned to be 2100 mm in length x 195 mm in height x 96 mm in width. The amount of mortar discharged was 0.02 liters/sec, and the nozzle movement speed was 40 mm/sec. The filaments were stacked so that they overlapped the previously printed filament by about 1 mm. Eventually, three rows were printed per layer to create a beam width of 96 mm, as shown in Fig. 2. In addition, a sodium silicate-based quick-setting agent was sprayed automatically on the printed filaments. Three specimens were made with and without reinforcing bars (hereafter referred to as reinforced and unreinforced specimens). For the reinforced specimen, SD345 D10 rebar was placed with a net cover of 45 mm from the bottom edge of the specimen. It was clarified that a rebar placed between the rows of filaments induce splitting cracks in the preliminary tests. After stacking up to three layers, the rebars with 45 mm cover spacers attached to both ends (outside the mortar specimen) were placed on the printed filaments, and then stacked up to 13 layers totally, as shown in Figs. 2 and 3. The prepared specimens were cured in air for 24 hours at room temperature of 20°C, then wet cured for 14 days, and then sealed cured in the same environment until the age of 27 days.

The cylindrical specimens having φ50×100mm for the compressive strength and splitting tensile strength tests were prepared by filling with the mixed mortar and curing it under the same conditions as the RC beams.

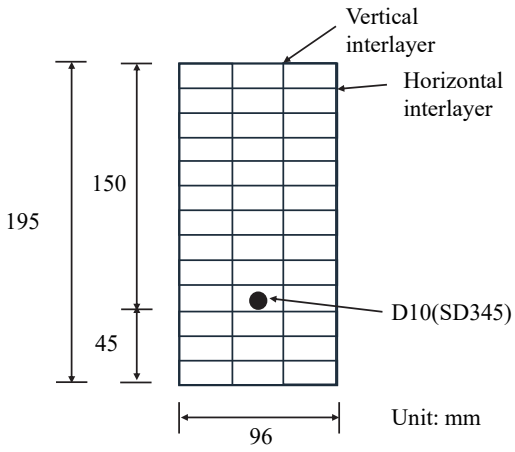

Figure 2: Cross section of beam and arrangement of filament.

Figure 3: Printed specimens.

2.4 Testing

The outline of the flexural test for reinforced and unreinforced beam specimens is shown in Fig. 4. The roller support was adopted to both ends. Flexural test with a constant moment span of 200 mm and loading span of 1800 mm was carried out. The load (load cell capacity 100 kN, sensitivity 30 N) and the displacement at both loading points (displacement transducer capacity 50 mm, sensitivity 1/200 mm) was measured. In

addition, to measure the axial strain at each beam height during loading, strain gauges (length 30 mm) were attached to the filaments (13 layers) on the side of the specimen center. In addition, a strain gauge was also attached to the upper surface to measure compressive strain.

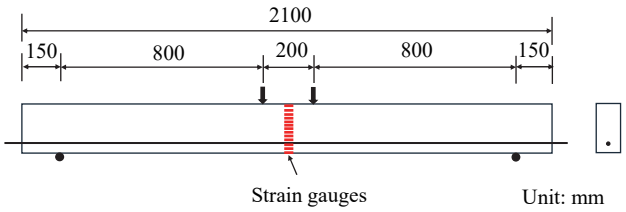

Figure 4: Flexural test condition.

2.5 Bond strength of interlayer

In order to investigate the effect of the horizontal interlayer bond strength on failure behavior of the beam specimen, the interlayer bond strength was measured. The attachment having the size of 40 x 40 mm was glued with unreinforced specimen (top and bottom surface) by using epoxy adhesive, as shown in Fig. 5. A notch was made with a concrete cutter up to the depth of target interlayer, and a tensile force was applied. Five specimens were prepared for each, and the maximum and minimum values by the tests were discarded, so that three data were used for an assessment.

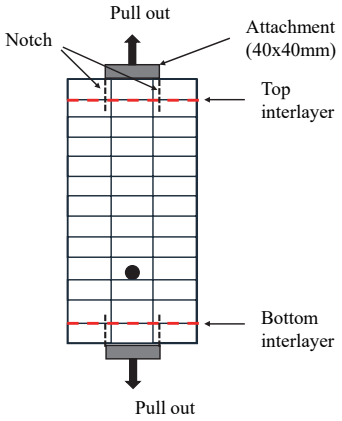

Figure 5: Test setup for bond strength test of interlayer.

3 EXPERIMENTAL RESULTS

3.1 Material test

The compressive strength of the mortar (27 days) using the cylindrical specimens are shown in Table 2, and the tensile strength of the reinforcing bars is also tabulated in Table 3.

Table 2: Results of material testing for mortar

	Compressive strength	Splitting tensile strength	Elastic modulus
Averaged (N/mm^2)	86.3	5.4	$33.5x10^3$
C.O.V(%)	6.0	8.0	6.0

* obtained from 3 mould specimens

Table 3: Results of material testing for rebar

Yield strength (N/mm^2)	Tensile strength (N/mm^2)	Elastic modulus (kN/mm^2)
86.3	5.4	202

* obtained from 4 specimens

3.2 Unreinforced specimens

The averaged maximum load was 5.55kN, with a coefficient of variation of 11%. Only a crack occurred in the center of the beam. The cross-sectional area of the specimen used to calculate the flexural strength was the maximum area connecting the convexities of each side. As a result, the averaged flexural strength was 3.65 N/mm^2. Figure 6 shows a part of fractured cross section after the test. There was no large void adjacent to layers or rows, and homogeneous hardened matrix was observed.

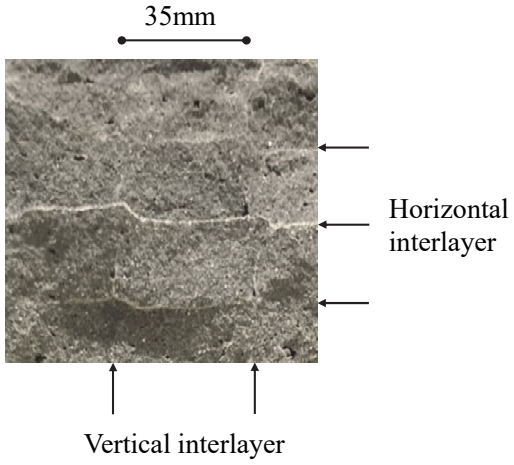

Figure 6: Interlayer.

3.3 Reinforced specimens

The load-displacement curves obtained

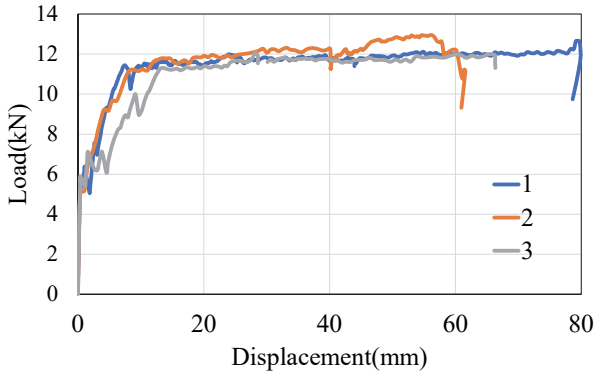

Figure 7: Load displacement curves.

from the flexural test of the reinforced specimens are shown in Fig. 7. The initial cracking load and ultimate load were 5.3 kN and 12.5 kN, respectively. Those were averaged values obtained from the three specimens. Figure 8 shows the crack patterns of the specimens at the end of the flexural test. For all reinforced specimens, flexural cracks occurred within the constant moment span mainly, and the maximum load was reached after the rebar yielded. After the initial cracking, the flexural cracks progressed upward as the load increased. Then, interfacial cracks (interlayer delamination) occurred along the rebar position.

As shown in Figs. 8 and 9, the shape of the cracks differed for each specimen, and in the No. 1 and 3 specimens, interlayer delamination occurred at the rebar position over the entire length of the loading span. At the end of the test, compression failure of mortar of the No.2 specimen was visually confirmed, and the failure behavior was similar to that of conventional RC beam.

Regarding the final stage for 3DCP specimens in this study, interlayer delamination due to compressive stress also observed in the first or second layer from the top of specimen. The failure mode with delamination, which occurred in the compression side, was one of the typical failure modes of the specimen fabricated by 3DCP technology.

3.4 Calculation of load carrying capacity

Using averaged values of the materials in Tables 2 and 3, the ultimate strength was calculated to be P_u=10.0kN. As mentioned above, the averaged strength obtained in this experiment was 12.6kN, so the experimental value was about 10% higher, and the conventional calculation method can be adapted for safe side.

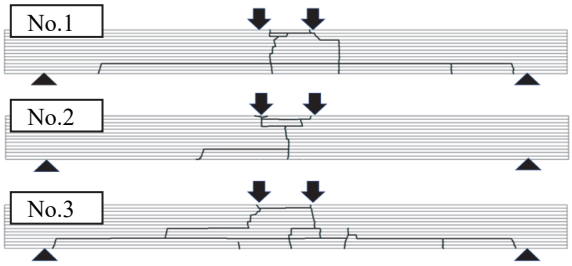

Figure 8: Crack patterns.

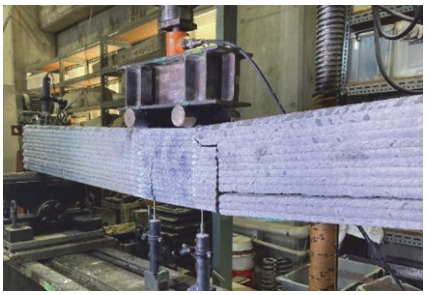

(a) No. 1 specimen with multiple cracks and delamination along rebar

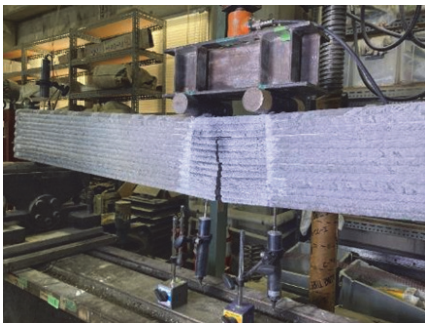

(b) No. 2 specimen with single crack

(c) No.1 specimen (close up)

Figure 9: Failure mode.

The strain on the filament side of each layer is plotted with the number of filament layers (1

to 13), as shown in Fig. 10. Regarding the behavior before and after cracking, the neutral axis of the beam specimen before cracking was located in the 7th layer. After cracking, the neutral axis shifted to the upper layer. This shows the same behavior as a conventional reinforced concrete beam, and it was clarified that compensation plane can be ensured before and after cracking. In other words, up to this load level, there was no slip in each interlayer.

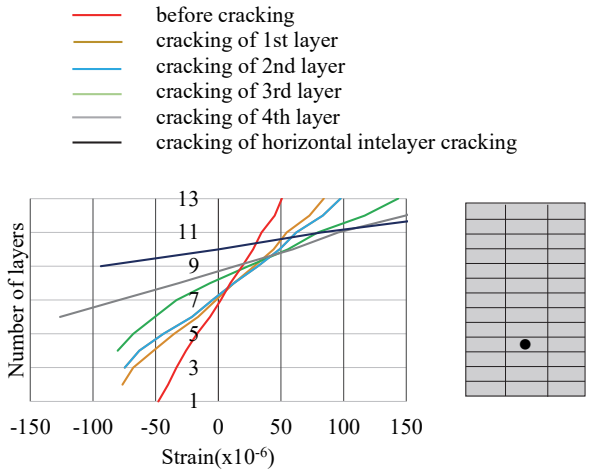

Figure 10: Strain distribution in cross section at each loading level.

Figure 11 shows the relationship between the compressive strain of the mortar at the top surface and the displacement at the loading point. For the No. 1 specimen, the maximum compressive strain was about 3,500 micron, and it finally entered the unloading process. It seems that the mortar different from the measurement position collapsed. For the No. 2 specimen, the strain suddenly decreased at a maximum compressive strain of about 2,900 micron. For the No. 3 specimen represented a very small value of about 1,100 micron compared to the compressive strain of the other specimens. It seems that interlayer delamination was dominant in failure behavior.

Figure 12 shows the compressive strain at the top surface of each specimen and the compressive strain at the sides of the first and second layers from the top (13th and 12th layers from the bottom). In both the No. 1 and No. 2 specimens, there was a large difference in strain between the top surface and the side of the 12th layer. It means that a strain

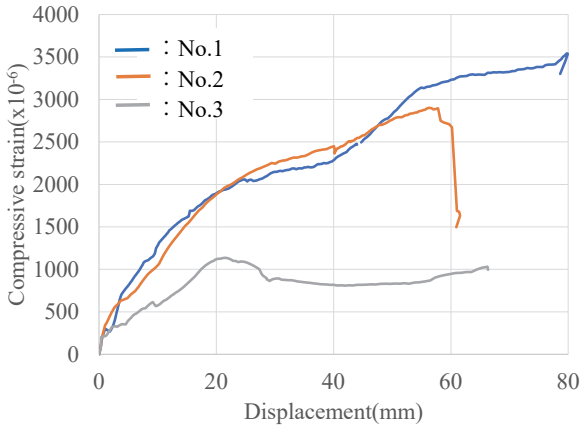

Figure 11: Compressive strain at upper surface of each specimen.

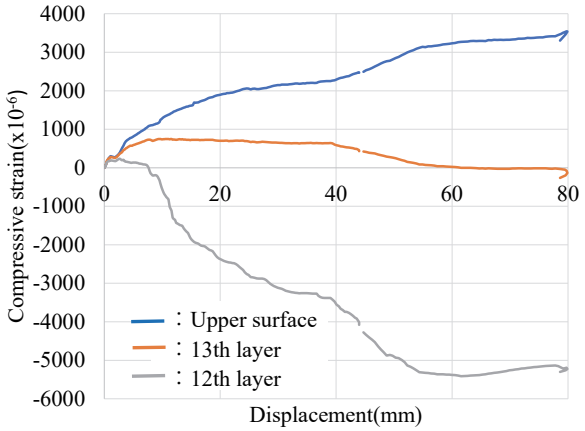

(a) No.1 specimen

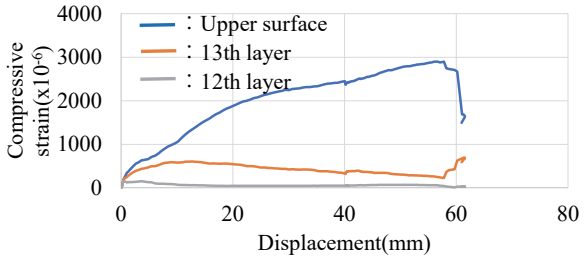

(b) No.2 specimen.

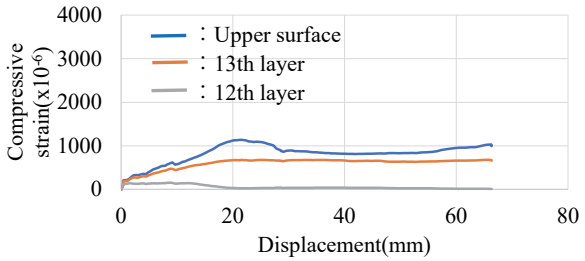

(c) No.3 specimen.

Figure 12: Compressive strain.

gradient occurred at the top layer.

On the other hand, in the No. 3 specimen, there was no difference in strain between the top surface and the first layer, and both strain values were significantly small. This is because delamination along a rebar was occurred, and tension stiffening becomes smaller than that of other specimens, as shown in Fig. 7.

In the 3DCP specimens, although there were many cracks depending on the interlayer delamination, larger energy consumption may be imparted to the beams, as shown in Fig. 7.

3.5 Interlayer bond strength

Using the unreinforced specimens after the flexural test, interlayer bond strength test was conducted, as shown in Fig. 5. Table 4 tabulates the obtained bond strength and Fig. 13 shows the delaminated interface. All fracture locations coincided with the interlayer locations.

The upper interlayer bond strength is about 20% lower than that of the lower layer. It seems that the lower interlayer bond strength increases because of the compaction due to stacking of upper layer during printing.

Table 4: Bond stregth at interlayer

	Bottom interlayer (between 1st and 2nd layers)	Top interlayer (between 12th and 13th layers)
Bond strength (N/mm^2)	1.7	1.4
C.O.V (%)	14	9

Figure 13: Fractured specimens for bond strength tests.

The strength ratio (interlayer bond strength in Table 4 / splitting tensile strength in Table 2) was about 30%. As shown in Fig. 6, a slightly white layer can be seen between the layers in the cross section. This is presumably a sodium silicate-based quick-setting agent sprayed during stacking to improve buildability. Quick hardened mortar of the filament surface may have some effect on the adhesion between layers. Further discussions are needed.

4 CONCLUSIONS

The following conclusions are obtained.

(1) Printed reinforced members exhibit ductile flexural failure behavior with flexural cracks within moment constant region, in addition to delamination of interlayer due to less bond properties.

(2) Before yielding of rebar, compensation plane was observed, and the effect of delamination of interlayer on flexural behavior was not significant.

(3) The estimation of load carrying capacity can be given as safety side.

REFERENCES

[1] Buswell, R.A., Leal de Silva, W.R., Jones, S.Z., and Dirrenberger, J., 2018, 3D printing using concrete extrusion: A roadmap for research, *Cement and Concrete Research*, 112: 37-49.

[2] Zhang, J., Wang, J., Dong, S., Yu, X. and Han, B., 2019. A review of the current progress and application of 3D printed concrete, Composites Part A, 125, https://doi.org/10.1016/j.compositesa.2019.105533

[3] Ogura, H., Hara, K., Yamamoto, S. and Abe, H., 2024, Flexural performance of fiber-reinforced 3D printed concrete beams with axial rebar, *Transforming Construction: Advances in Fiber Reinforced Concrete (BEFIB 2024)*, RILEM Bookseries, Vol 54. Springer Dresden, Germany, 475-483.

[4] Miyajima, A. Toh, S. and Kunieda, M., Compressive Strength of Extruded Filaments by 3D Printer, *2023 International Conference on Unmanned System Applications*, July 13, 2023, Shizuoka, Japan.